

COMPUTATION OF STRESS INTENSITY FACTORS FOR NOZZLE CORNER CRACKS BY VARIOUS FINITE ELEMENT PROCEDURES

M.J.G. BROEKHOVEN

*Laboratory for Thermal Power and Nuclear Engineering,
Delft University of Technology, Delft, The Netherlands*

SUMMARY

Introduction

Application of linear elastic fracture mechanics, requiring the determination of crack tip stress intensity factors (K -factors), is recommended in the ASME pressure vessel code (Section III, 1974 edition, Appendix G) for protection against non-ductile failure of nuclear pressure vessels. Due to the high local stresses associated with nozzle-to-cylinder junctions these areas deserve special concern in a fracture safety analysis. The complexity of both geometry and stress distribution at nozzle junctions seems to exclude the derivation of exact analytical solutions for K -factors and to indicate the application of the finite element technique as the prime approach for obtaining reliable values. The present study aims at deriving accurate K -factors for a series of 5 elliptical nozzle corner cracks of increasing size by various finite element procedures, using a three-level recursive substructuring scheme to perform the computations in an economic way on an intermediate size computer (IBM 360/65 system). A nozzle on a flat plate has been selected for subsequent experimental verification, this configuration being considered an adequate simulation of a nozzle on a shallow shell. The experimental results are presented in a companion paper to this conference.

Method of analysis

The computations have been performed with the ASKA finite element system using mainly HEXEC-27 (incomplete quartic) elements. The geometry has been subdivided into 5 subnets, with a total of 3515 nodal points and 6250 unknowns, two main nets and one hyper net. Each crack front is described by 11 nodal points and all crack front nodes are inserted in the hyper net, which allows for the realization of the successive crack geometries by changing only a relatively small hyper net (615 to 725 unknowns). Output data have been interpreted in terms of K -factors by the global energy method, the displacement method and the stress method. Besides, a stiffness derivative procedure, recently developed at Brown University, which takes full advantage of the finite element formulation to calculate local K -factors, has been applied. Finally it has been investigated whether sufficiently accurate results can be obtained by analyzing a considerably smaller part than one half of the geometry (as strictly required by symmetry considerations), using fixed boundary conditions derived from a far cheaper analysis of the uncracked structure.

Results

Some significant results are:

- inserting all crack front nodes in the (small) highest level net yields a considerable reduction of computation time;
- the stiffness derivative procedure yields the most reliable local K -values;
- the stress method is not applicable; the displacement method yields some acceptable local K -values. Considerable increase in accuracy is obtainable by using modified elements at the crack fronts;
- local K -factors vary up to about 50% along the crack fronts;
- average values of K -factors per crack front as obtained by the displacement method and the stiffness derivative procedure agree very well with the global energy method results and available experimental data for crack depths between 0.1 and 0.4 times the plate thickness;
- restricting the analysis to a 45° instead of a 180° segment with fixed boundary conditions causes less than 7% deviation for crack depths up to 0.4 times the plate thickness.

1. INTRODUCTION

Because the peak stresses associated with nozzle junctions considerably promote crack extension in these regions, nozzle corner cracks and in particular those located in a plane through the axes of nozzle and cylindrical shell (fig. 1), constitute one of the main areas of concern regarding the fracture safety of LWR pressure vessels.

The linear elastic fracture mechanics (LEFM) based approach adopted in App. G of the ASME Code, Section III [1] to ensure safety against non ductile fracture, requires the determination of stress intensity (K-) factors for (postulated) defects under all relevant conditions. Whereas this Appendix provides definite procedures for calculating K-factors for cracks in less complicated geometries, no such procedures are given for nozzle corner cracks. Reference is made to an approximation procedure provided in WRC Bulletin 175 [2], based on results from a finite element analysis [3] and experimental data from burst tests on epoxy model vessels [4].

While a minimum number of parameters suffices to describe the configuration of the App. G "design defect" located at the surface of a spherical or cylindrical vessel wall and the stress distribution in such a wall due to pressure and thermal loading, thus allowing for a rather simple graphical presentation of the influence of these parameters on the relevant K-factor, the much larger number of parameters governing the nozzle corner crack problem will considerably hamper or may even rule out the accurate application of such a procedure. Values of the several geometrical parameters involved, such as inside and outside corner radii, inside and outside tapers, wall thicknesses and diameters of both nozzle and vessel, vary considerably with the various nozzle designs applied in practice, each combination of these geometrical parameters being associated with a specific complicated stress distribution. The influence of the geometry of the nozzle-to-cylinder configuration on the resulting K-factors for corner cracks may be illustrated by comparing the K-factors established for rather deviating geometries as provided in fig. A5-1 of [2]; results of experiments carried out with considerable multiplicity on 2 different geometries [4] show clear mutual deviations, while these experimental results exceed the finite element results for another (for BWR vessels more representative) geometry [3] by over 60%. Experimental results obtained by a quite different technique (photoelasticity) [5] for another geometry also seem to support the significant influence of the geometry. The experimental results, however, concern geometries that are not very typical for present LWR designs so that this significant influence does not exclude a priori that commonly used LWR designs can be classified in such a way that simplified standard procedures for K-factor determination can be applied without unacceptable loss of accuracy. (The statement in App. G that the design defect size in nozzle corners may be a fraction of that postulated for the vessel shell, which seems in agreement with the results of a provisional study on the basis of work performed at the author's laboratory [6], indicates that simplified conservative approximations are inadequate here.) However, this requires much more data (both accurate theoretical and experimental results for the same geometries) than available at present. (Except for the studies mentioned above work is in progress within the HSST-program [7]; other experimental studies carried out on steel pressure vessel, a.o. [8-10], as yet seem to

lack a sufficiently firm LEFM basis to be used for the purpose of comparison)*. A.o. based on these considerations the nozzle corner crack problem has been adopted as the main area of research within a Dutch cooperative research program [11]. Activities within this program comprise a.o. experimental investigations, evaluation of the applicability of simplified analytical approximations and development of a more advanced semi-analytical procedure (provisional results on these subjects have been presented previously [12] whereas recent results are treated in a companion paper to this conference [13]) as well as 3-D finite element computations reported here. For reasons of comparison the f.e. computations concern the same nozzle-on-flat-plate model as chosen for the experiments (see [13]).

2. ANALYSIS

2.1. GENERAL INFORMATION

The model investigated (a scale 1:4 model of the main coolant inlet nozzle of the Dutch Dodewaard 50 MWe BWR vessel) is shown in fig. 2. Whereas most computations concern uniaxial (1:0) loading, similar to the experiments, a separate run was made for the case of biaxial (1:½) loading. This biaxially loaded nozzle-on-flat-plate configuration constitutes an accurate simulation of the real nozzle-on-pressurized cylinder configuration [14,15]. The maximum membrane stress perpendicular to the crack plane is 1 N.mm^{-2} . $E = 20.7 \times 10^4 \text{ N.mm}^{-2}$, $\nu = 0.3$.

All computations have been performed using the ASKA system (version 5.1) [16] as installed on the intermediate size computer (IBM 360/65) available at that time at the Delft University's Computing Center.

2.2. CHOICE OF THE MESH; SUBSTRUCTURING

Factors that were instrumental in choosing the mesh for the plane containing the cracks ($\psi=0$, figs. 2 and 3) at the very start of the investigations were:

- the mesh should allow for the analysis of a series of 5 cracks of increasing size;
- applicability of the displacement and/or stress method (f.e. [17]) and possibly other methods to obtain local K-factors, next to application of the global energy method [3,17] to obtain K-values averaged along the crackfronts.

Because early investigations by a semi-analytical procedure [12] indicated a strong θ -dependency of the K-factors, a minimum of 5 elements along each crackfront seemed required. Application of higher order elements as available within the ASKA system (HEXEG 27, incomplete quartic with parabolic curved edges) was necessary to approximate the singular crack tip stress and displacement fields (incorporation of special crack tip elements (like [18]) in the ASKA system seems hardly attainable by a user; the

*Upon completing this paper the author's attention was drawn at two further very recent finite element studies [25,26], the results of which qualitatively seem to compare well with the finite element results reported here.

possibility to modify existing elements in singularity elements through a simple midside node translation [19,20] (appeared much later in literature). The 5 crackfronts described by the resulting mesh of fig. 3 are equal to those observed at the fatigue experiments [13] (fig. 2).

A much coarser mesh, containing only 17 elements to describe the part of the section shown in fig. 3, has been applied for regions remote from the crack area. PENTAC 18 elements (incomplete cubic, parabolic curved edges) were used for the transition from fine to coarse mesh.

The resulting total number of over 6000 unknowns in relation to the capacity of the available computer facility necessitated the use of a substructuring option, available within the ASKA system. The three level substructuring schematization shown in fig. 4 was selected partially on the basis of practical considerations, a.o. regarding allowable job sizes. However, instrumental in the choice of the hypernets (100...600) was the fact that such choice yielded the opportunity to analyse 6 geometries (1 uncracked and 5 with cracks of step-wise increasing size) by only changing the relatively small hypernet (about 670 unknowns vs. 2019 in subnet 1) through inserting all crack surface nodes in this hypernet. This yielded a considerable reduction in total computation costs.

Details of the computational procedures and techniques, with particular reference to mesh generation, recursive substructuring and computational costs, are described in [21] so that these subjects will only be summarized here in short.

2.3. MESH GENERATION AND PLOT PROCEDURES

Because of symmetry with respect to the plane $y=0$ only one half of the structure had to be analysed. All nodal points are located in radial planes, denoted ψ -planes (fig. 2). This permitted generation of all nodal point coordinates in the $\psi=0$ plane using a series of hand made topological schemes. Subsequent rotation from the $\psi=0$ plane to the appropriate ψ -plane, resulting in appropriate X,Y,Z coordinates, was performed with a special computer program. Both 2-D plots for sections through the structure (f.e. fig. 3) as well as isometric plots (where necessary containing only a few selected elements) were made to check the topology.

2.4. COMPUTATION PROCEDURES

Because the multi-level recursive substructuring technique was a non-standard ASKA facility at the beginning of the analysis, a control program (as generally required for ASKA-computations and denoted ASKA Processor Control Program (APC)) for this technique has been drawn up and extensively tested on a dummy structure. With this APC program the computations for the present problem were carried out in a series of separate jobs. After completion an evaluation of the computation times required allowed for indicating guidelines for a more optimal substructuring schematization, such as preferably ≤ 1000 internals per subnet, a maximum of 600 externals per subnet, restriction of mainnet sizes and utmost limitation of the size of the ultimate hypernet, if necessary by the use of four levels.

Application of these guidelines may lead to well over 50% savings in computation times [21].

2.5. ANALYSIS OF A SEPARATE SMALL PART OF THE STRUCTURE

The disturbance of stresses and displacements due to the introduction of a crack damps out with the distance from the cracked region; so that in general a surface remote from and enclosing this region can be determined where these parameters are almost unaffected by the crack.

An analysis of the enclosed region only, with boundary conditions (stresses, displacements) derived from an analysis of the uncracked structure then yields almost the same results as obtainable from an analysis of the entire structure, but at lower costs. The loss of accuracy inherent to such a procedure may be roughly estimated within an analysis of the entire structure from the proportional change of the stresses and/or displacements at the prospect boundaries due to introduction of the crack.

For this purpose the change of displacements due to the introduction of cracks of step-wise increasing size (cracks 1 thru 5, fig. 2) has been calculated for the planes $\psi = 16^\circ$, 45° and 90° respectively as well as for the planes $x^2 + y^2 = (0,5d + 36,25 \text{ mm})^2$ ($d =$ inside nozzle diameter) and $z = 30 \text{ mm}$, with $\psi \leq 45^\circ$ for both latter cases (see fig. 5). For practical reasons these planes, selected as prospect boundary planes for the analysis of a small part of the structure, all are simply shaped boundary planes between elements. Maximum changes (average changes being considerably lower) turned out to be (for cracks 1...5 respectively)

0.29, 6.15, 32.3 ...percent for the $\psi = 16^\circ$ plane,

0.03, 0.57, 3.45, 14.6 and 43 percent for $\psi = 45^\circ$,

..., 3.83 and 12.8 percent for $\psi = 90^\circ$,

with lower values for the other planes.

This indicated that the analysis could have been restricted to one quarter of the plate (x and $y \geq 0$) for cracks up to the depth of crack nr. 4, and that a separate analysis of the part of the structure shown in fig. 5 might yield K-values for the first 3 cracks that are in close agreement with those obtained by the former analysis of the entire structure. A separate analysis was performed for this part of the structure, loaded on its interfaces with prescribed displacements as obtained from the analysis of the entire uncracked structure. (Evidently, by application of fixed prescribed displacements the true K-factors will be underestimated, whereas fixed prescribed stresses (nodal loads) will yield an overestimation. The procedure of prescribed displacements was chosen in order to obtain an idea about its un-conservatism.) The analysis required generation of two new subnets (A and B instead of 1 and 2, fig. 5) and a new mainnet 10; the finite element schematization within the new subnets was equal to the original schematization. Total computer costs involved in this analysis were less than one quarter of those for the original analysis. Results are presented in section 3.

2.6. DERIVATION OF K-FACTORS

- Stress and displacement methods.

These require substitution of the nodal stresses or displacements that result from the finite element analysis in eqs. (1a) and (1b) resp., and extrapolation to $r=0$; stresses and displacements perpendicular to the crack plane for $\varphi = 0^\circ$ and 180° respectively have been used (x, y, z are local coordinates).

$$K_{r \rightarrow 0} = \sigma_{x,y} \cdot \sqrt{2\pi r} \cdot f_{x,y}(\varphi) \quad (1a)$$

$$K_{r \rightarrow 0} = u_{x,y} \cdot \frac{E}{4(1-\nu^2)} \cdot \sqrt{\frac{2\pi}{r}} \cdot f_{x,y}(\varphi, \nu) \quad (1b)$$

where

- K = stress intensity factor
- $\sigma_{x,y}$ = stress components
- $u_{x,y}$ = displacement component
- r, φ = polar coordinates
- E = Young's modulus
- ν = Poisson's constant
- x,y = Cartesian coordinates
- f = goniometrical functions.

- Global energy method.

This method is based on the LEFM relation (assuming plane strain):

$$(\pm) \frac{dU}{dA} = G = \frac{K^2 (1-\nu^2)}{E} \quad (2)$$

where

- U = strain energy within the structure
- A = area of the crack surface
- G = strain energy release rate
- + = for prescribed external loads
- = for prescribed external displacements.

By releasing the prescribed y-direction degree of freedom of nodes in the crack plane the crack surface is increased step by step; U can be readily calculated for the uncracked and 5 cracked configurations from the displacements of externally loaded nodes by

$$U_i = \sum_{n=1}^m \frac{1}{2} P_n u_{n_i} \quad (3)$$

where

- P = nodal force,
- u = nodal displacement in the loading (Y-)direction,
- n = 1,...,m = number of externally loaded node,
- i = 0,1...5 indicates uncracked geometry and geometry with cracks
1,...,5 respectively.

(ΔU has also been calculated from forces and displacements of nodes located in the crack plane; this yielded identical results).

Derivation of G, and thus of K, from the resulting U (or ΔU) and A data has been performed by substituting the finite differences $\Delta U/\Delta A$ in eq. (2). This straight forward procedure avoids the introduction of unknown errors that result if some arbitrary curve (f.e. polynomial) is forced through the set of (U_i, A_i) data and subsequently differentiated to obtain the differential dU/dA (results of this latter procedure indeed turned out to be

highly dependent on the polynomial chosen).

- Stiffness derivative procedure.

Taking full advantage of the finite element formulation (i.e. writing eq. (2) in finite element method's terminology) Parks [22] developed an optimal procedure for application of the LEFM "energy method" within a finite element analysis. He showed that the change of potential energy associated with an alteration of the crack front can be calculated from the vector of displacements for the original cracked configuration (to be obtained by a normal stress analysis run) and the change of the stiffness matrix of a ring of elements surrounding the disturbed part of the crackfront due to the alteration.

For the present 3-D crack configuration this means that, if a single node on the crack front is given a displacement $\Delta \epsilon_0$ normal to the crack front and in the crack plane, so that neighbouring points at a position s along the crack front obtain a translation $\Delta \epsilon(s)$, $G(s)$ (and thus $K(s)$, using eq. (2)) can be solved from the equation

$$-\Delta P = -\frac{1}{2} \{u\}^T \Delta [K] \{u\} = \int_s G(s) \Delta \epsilon(s) ds \quad (4)$$

where

- P = potential energy
- {u} = vector of nodal displacements
- [K] = global stiffness matrix
- T = transpose
- ℓ = crack length
- G = strain energy release rate
- s = position along the crack front

The only contribution to $\Delta [K]$ stems from a group of deformed elements enveloping the displaced nodal point, which may be contracted to the few elements containing this node, as applied in the present study. The right hand member of (4) has been calculated by numerical integration.

Because the resulting $G(s)$ or $K(s)$ values are sensitive to the amount of local crack front distortion relative to crack length and element size, appropriate values of $\Delta \epsilon_0$ have been taken from a trial and error procedure using guidelines provided in [22].

3. RESULTS, DISCUSSION AND CONCLUSIONS

K-factors resulting from the various computation procedures are presented in figs. 6 and 7, together with some analytical and experimental results [13]. The stress method yielded strongly deviating results and was considered inapplicable for this analysis, so its results are omitted.

Fig. 6 shows the variation of K along the crackfronts (i.e. as a function of θ). The results of the stiffness derivative procedure (analysis of one half of the structure, uniaxial loading) are shown in all 4 sections of this figure as a basis for comparison. The qualitative agreement between the results of the several procedures, and thus the obviousness of a strong K-factor variation along the crackfronts, is evident.

Fig. 7 shows K values averaged along the crackfronts vs. average crack depth. It should be

remarked that the experimental results, also included in this figure as a line indicating average values, showed no significant K-variation along the crack fronts [13].

Comparison yields the following conclusions.

- Results of the global energy method and average values of the stiffness derivative procedure are in close mutual agreement and compare very well with the experimental results.
- Results of a semi-analytical procedure [13], averaged per crackfront, compare very well with the aforementioned f.e. and experimental results for crack depths up to about 12 mm (i.e. the crack depths of main concern in nuclear applications), which supports the practical applicability of this relatively very cheap procedure. Its results show approximately the same θ -dependency of the K-factor as the results of the stiffness derivative procedure for crack numbers 1 through 3.
- Results of the displacement method, though too low for the whole range of crack sizes investigated, show reasonable agreement with the aforementioned results for cracks of intermediate depth (about 5 to 10 mm).
- Analysis of a suitably chosen small part of the structure, with fixed boundary conditions (loads, displacements) obtainable from a much cheaper f.e. analysis of the uncracked structure (f.e. [14, 15]), yields results of sufficient accuracy (in the present analysis within a few percents for the crack depths of concern) at much lower costs.
- Results obtained by the stiffness derivative procedure for the cases of uniaxial (1:0) and biaxial (1:0.5) loading (fig. 6) show a very good qualitative agreement regarding the K-factor variation along the crackfronts. K-factors for the biaxial case are about 10% lower. This agrees well with the difference in stress level for the stresses perpendicular to the crack plane in the uncracked situation.
- Experimentally observed fatigue crack growth rates do not reflect by far the calculated strong variation of K along the crack fronts. Results of refined analytical treatments of cracks intersecting free surfaces indicate boundary layer effects such as an abrupt drop-off of the K value [23] and a change of the character of the singularity [24]. Being restricted to a small boundary layer these phenomena, however, probably yield only a minor contribution to the explanation of the discrepancy indicated above. Crack closure may play a role; the greater crack tip plasticity near the free surfaces promotes crack closure and may reduce the effective part of the K-factor and thus the fatigue crack growth rate there.

The fact that K-factors obtained from burst tests on epoxy models [4] considerably exceed the calculated K-factors from [3] (in fact averaged values along the crack fronts), as mentioned in the introduction, might to some extent be attributed to the strong K-factor variation; fracture of the rather brittle models may have initiated at the location of the maximum K-value which is considerably higher than the average value. For real LWR pressure vessel nozzles the problem seems even more complicated because next to the K-factor variation, high gradients of both fracture toughness and constraint are involved. Whether for these configurations an average value of the K-factor is an appropriate parameter in an ASME III App. G-type fracture analysis seems to require further investigations.

ACKNOWLEDGEMENTS

The work reported here has been carried out at the author's laboratory within the framework of the Dutch cooperative research program BROS [11], partly sponsored by the Dutch Ministry of Economic Affairs with Rotterdam Dockyard Company as main contractor.

The considerable efforts of graduate students who participated in this work have been much appreciated. Contributions by his colleagues Mr. M.G. van de Ruijtenbeek and Mr. H.A.C.M. Spaas are thankfully acknowledged, where the latter was especially involved in continuous support regarding the use of the ASKA system and the elaboration of its multi-level substructuring option.

REFERENCES

- [1] ASME Code, Sect. III, App. G (1974 ed.)
- [2] WRC Bulletin 175, Aug. 1972.
- [3] GILMAN, J.D., RASHID, Y.R.: 1st SMiRT, paper G2/6, 1971.
- [4] DERBY, R.W.: Exp. Mech., Dec. 1972, pp. 580/4.
- [5] RUIZ, C.: "Strain", Jan. 1973.
- [6] BROEKHOVEN, M.J.G.: present. for "Groupe Fragilité Rupture", Winterthur, 1974.
- [7] DERBY, R.W., MERKLE, J.G. et al.: HSST Program, rep. ORNL-4895, Feb. 1974.
- [8] DECOCK, J.: 1st ICPVT, paper II-58, 1969.
- [9] PICKETT, A.G., GRIGORY, S.C.: WRC Bulletin 135, Nov. 1968.
- [10] FUJIMURA, T. et al.: 2nd ICPVT, paper II-58, 1973.
- [11] BROEKHOVEN, M.J.G.: rep. MMPP-84, Delft Un. of Techn., Lab. for Nucl. Engng., Dec. 1973.
- [12] BROEKHOVEN, M.J.G.: 2nd SMiRT, paper G4/7, 1973.
- [13] BROEKHOVEN, M.J.G., RUIJTENBEEK, M.G. v.d.: 3rd SMiRT, paper G4/7, 1975.
- [14] CAMPEN, D.H. van: Thesis, Delft Un. of Techn., May 1972.
- [15] CAMPEN, D.H. van, SPAAS, H.A.C.M.: Nucl. Eng.&Design, Vol. 21, 1972, p. 368.
- [16] SCHREM, E., ROY, J.R.: IUTAM Coll., Liège, Aug. 1970.
- [17] CHAN, S.K., TUBA, I.S., WILSON, W.K.: Eng. Fract. Mech., Vol. 2, 1970, pp. 1/17.
- [18] TRACEY, D.M.: Int. J. Fract., Vol. 9, 1973, p. 340.
- [19] BARSOUM, R.S.: Int. J. Fract., Vol. 10, 1974, p. 603.
- [20] NEALE, B.K.: Int. J. Fract., Vol. 11, 1975, p. 177.
- [21] BROEKHOVEN, M.J.G., SPAAS, H.A.C.M.: rep. MMPP-101, Delft Un. of Techn., Lab. for Nucl. Engng., Aug. 1974 (presented at IKOSS Baden-Baden Cong., Nov. 1974).
- [22] PARKS, D.M.: Techn. Rep. NASA NGL 40-002-080/13, Div. of Eng., Brown Un., May 1973.
- [23] HARTRANFT, R.J., SIH, G.C.: in "Meth. of Anal. and Solution of Crack Problems", Noordhoff, 1973.
- [24] BENTHEM, J.P.: to be published.
- [25] HELLEN, T.K., DOWLING, A.R.: Int. J. PVP (3), 1975.
- [26] SCHMITT, W.: to be published.

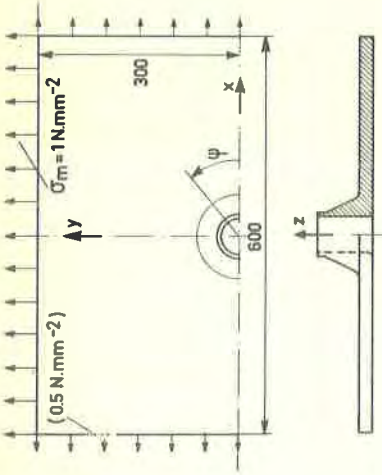


Fig. 1. Nozzle-to-cylinder junction with corner crack

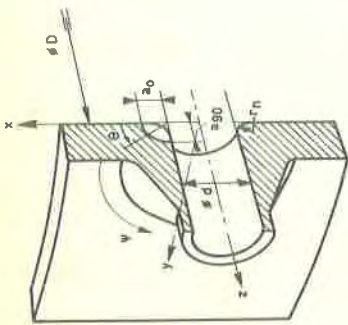


Fig. 2. Nozzle N5 on flat plate model

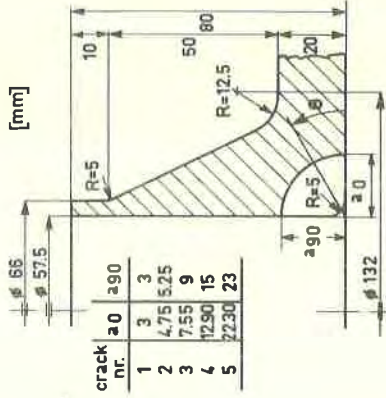


Fig. 3. Finite element schematization in $\psi=0$ -plane (with crackfronts)

crack nr.	a	a/90
1	3	3
2	4.75	5.25
3	7.55	9
4	12.90	15
5	22.30	23

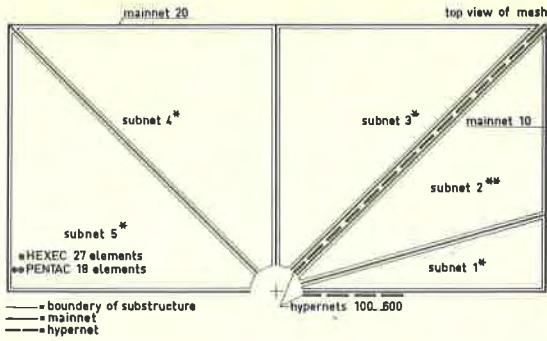


Fig. 4. Schematization in subnets, mainnets and hypernets

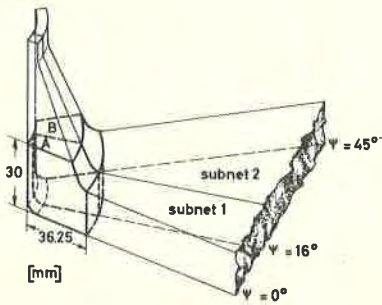


Fig. 5. Part of the structure treated in a separate analysis

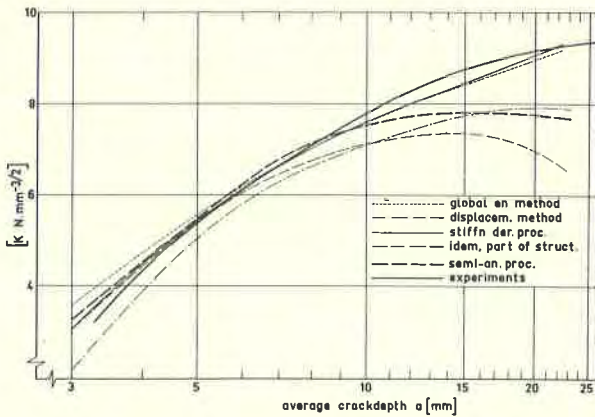


Fig. 7. Comparison of nozzle corner crack K-factors (averaged along the crack fronts) from various procedures

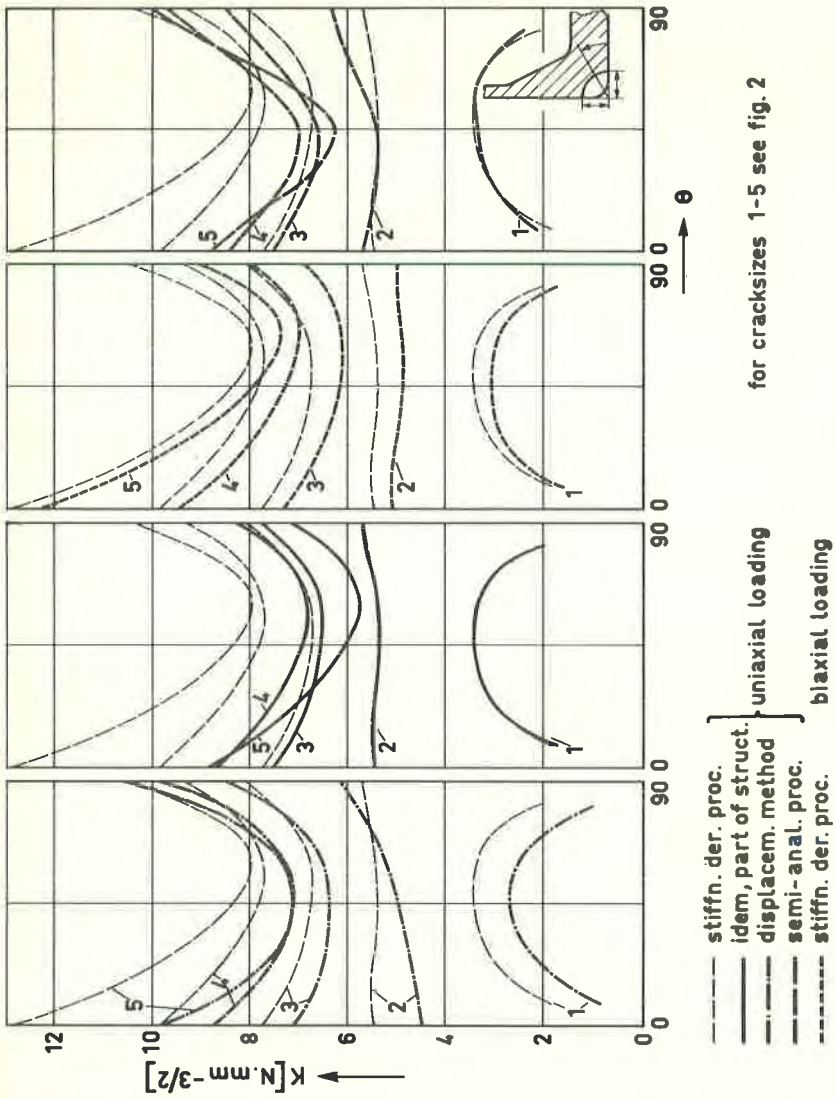


Fig. 6. Comparison of nozzle corner crack k-factors (as function of θ) from various procedures